

1 **Ancient DNA and microfossils reveal dynamics of three harmful**  
2 **dinoflagellate species off Eastern Tasmania, Australia, over the**  
3 **last 9,000 years**

4

5 Linda Armbricht<sup>1\*</sup>, Bradley Paine<sup>2</sup>, Christopher J.S. Bolch<sup>3</sup>, Alan Cooper<sup>4</sup>, Andrew  
6 McMinn<sup>2</sup>, Craig Woodward<sup>5</sup> and Gustaaf Hallegraeff<sup>2</sup>

7

8 <sup>1</sup> Australian Centre for Ancient DNA, School of Biological Sciences, Faculty of Sciences,  
9 The University of Adelaide, Adelaide SA 5005, Australia

10 <sup>2</sup> Institute for Marine and Antarctic Studies, University of Tasmania, Private Bag 129, Hobart  
11 TAS 7001, Australia

12 <sup>3</sup> Institute for Marine and Antarctic Studies, University of Tasmania, Locked Bag 1370,  
13 Launceston TAS 7250, Australia

14 <sup>4</sup> South Australian Museum, Adelaide, SA, Australia

15 <sup>5</sup> Australian Nuclear Science and Technology Organisation, Locked Bag 2001, Kirrawee DC  
16 NSW

17 \*Correspondence: [linda.armbricht@adelaide.edu.au](mailto:linda.armbricht@adelaide.edu.au)

18

19 **Highlights**

- 20 • Dinocyst and *sedaDNA* analyses were applied to marine sediments off Tasmania  
21 • *Alexandrium catenella* has been endemic to Australia for at least ~9,000 years  
22 • Recent *A. catenella* blooms are likely induced by climate and oceanographic change  
23 • *Gymnodinium catenatum* cysts in recent (~30y) sediments confirm a 1970s  
24 introduction  
25 • *Noctiluca scintillans* *sedaDNA* in recent (~30y) sediments matches a 1994  
26 introduction

27

28

29

30 **Abstract**

31 Harmful algal blooms (HABs) have significantly impacted the seafood industry along the  
32 Tasmanian east coast over the past three decades, and are expected to change in frequency  
33 and magnitude due to climate change induced changing oceanographic conditions. To  
34 investigate the long-term history of regional HABs, a combination of palynological and  
35 sedimentary ancient DNA (*sedaDNA*) analyses was applied to marine sediment cores from  
36 inshore (up to 145 years old) and offshore (up to ~9,000 years) sites at Maria Island,  
37 southeast Tasmania. Analyses focused Paralytic Shellfish Toxin (PST) producing  
38 dinoflagellates *Alexandrium catenella* and *Gymnodinium catenatum*, and the red-tide

39 dinoflagellate *Noctiluca scintillans*, which were specifically targeted using a hybridization  
40 capture *sed*aDNA technique. Identification of primulin-stained *A. catenella* cysts throughout  
41 the inshore sediment core, together with *sed*aDNA evidence of a bloom-phase of  
42 *Alexandrium* ~15 years ago, indicates recent stimulation of a cryptic endemic population.  
43 Morphologically similar but unstained *Alexandrium* cysts were observed throughout the  
44 offshore core, with *sed*aDNA confirming the presence of *A. catenella* from ~8,300 years ago  
45 to present. *Gymnodinium catenatum* cysts were detected only in inshore surface sediments  
46 from 30 years ago to present, supporting previous evidence of a 1970s introduction via  
47 shipping ballast water. *sed*aDNA confirmed the presence of *G. catenatum*-related sequences  
48 in the inshore and offshore cores, however, unambiguous species identification could not be  
49 achieved due to limited reference sequence coverage of *Gymnodinium*. Our hybridization  
50 capture *sed*aDNA data also confirmed the historically recent dispersal of the non-fossilizing  
51 dinoflagellate *Noctiluca scintillans*, detected inshore from ~30 years ago, matching first  
52 observations of this species in Tasmanian waters in 1994. At the offshore site, *N. scintillans*  
53 *sed*aDNA was detected only in surface sediments, confirming a recent climate-driven range  
54 expansion this species. This study provides new insights into the distribution and abundance  
55 of three HAB species in the Tasmanian region, including clues to past bloom phases. Further  
56 research into paleo-environmental conditions and paleo-community structure are required to  
57 identify the factors driving bloom phases through time and predict plankton community  
58 responses under different future climate scenarios.

59

60 **Key words:** dinoflagellate; biotoxin; ballast water; ancient DNA; seafloor; Australia

61

62 **Abbreviations:** harmful algal bloom, HAB; heuristic operations for pathogen screening,  
63 HOPS, hydrofluoric acid, HF; internally transcribed spacer, ITS; sedimentary ancient DNA,  
64 *sed*aDNA; small subunit ribosomal rRNA, SSU; large subunit ribosomal rRNA (LSU)

65

## 66 1 Introduction

67 The issue of whether harmful algal blooms (HABs) are increasing in extent and frequency  
68 due to climate change and the potential role of eutrophication and anthropogenic transport,  
69 remain hotly debated topics (Hallegraeff et al., 2021). When novel bloom phenomena impact  
70 on tourism, aquaculture, fisheries and human health, questions arise as to whether these  
71 blooms are the result of a recent species introduction into the area or of a cryptic endemic  
72 species' massive growth that is newly stimulated by changing environmental conditions.  
73 Much research has been undertaken deciphering the association of new algal bloom  
74 phenomena with human-assisted ballast water introductions (McMinn et al., 1998) or extreme  
75 climate events (Trainer et al., 2019). In contrast, very few studies have attempted to prove the  
76 'always-been-there, but previously-overlooked' scenario. To date, only a few studies have  
77 analysed long-term, *i.e.*, thousands of years, dynamics of harmful algal bloom species or the  
78 timing and mode of introduction to a region (*e.g.*, Thorsen et al., 1995, for *Gymnodinium*

79 *nolleri* (as *G. catenatum*) in Scandinavia; Klouch et al., 2016, for *Alexandrium minutum* in  
80 the Bay of Brest).

81 The ocean environment off eastern Tasmania is well documented as a climate change hotspot,  
82 characterized by a strengthening East Australian Current and rapidly increasing ocean  
83 temperatures (2.3 °C increase since the 1940s, Ridgway and Hill, 2009). The consequences of  
84 this rapid change are now being detected in coastal marine communities, including changes in  
85 plankton and HAB species composition (Thompson et al., 2009, Condie et al., 2019). A  
86 planktonic HAB example is the dinoflagellate *Gymnodinium catenatum*, a Paralytic Shellfish  
87 Toxin (PST) producer thought to be introduced to Tasmania in the 1970s by shipping ballast  
88 water. This species appeared noticeably in the mid-1980s, causing PST contamination up to  
89 250x acceptable limits and extensive shellfish farm closures in the Derwent-Huon estuaries  
90 from 1986 to 1993. After most shellfish farming in the area went bankrupt, the local  
91 government declared the area unsuitable for bivalve aquaculture. Supporting evidence for its  
92 introduction includes cysts detected in ships ballast tanks (Hallegraeff and Bolch, 1992),  
93 cysts evidence from marine sediment core analysis (McMinn et al., 1998), reproductive  
94 compatibility studies (Blackburn et al., 2001) and molecular genetic evidence (Bolch and de  
95 Salas, 2007).

96 The regional appearance and increase of other HAB phenomena have in contrast been  
97 attributed to climate-driven range expansion; exemplified by the dinoflagellate *Noctiluca*  
98 *scintillans*. Highly visible red tides and bioluminescent spectacles caused by *Noctiluca* were  
99 first documented in Australia from Sydney Harbour in 1860 (Bennett, 1860), have been more  
100 frequently reported since the 1990s, and even caused temporary closure of popular Sydney  
101 tourist beaches (Hallegraeff et al., 2020). Amongst the causes of *N. scintillans* blooms are  
102 eutrophication, upwelling and ocean circulation (Dela Cruz et al., 2002, 2003). *Noctiluca* was  
103 first observed in Tasmania in 1994, carried south by the East Australian Current, and  
104 representing a new threat to the expanding salmonid fish farm industry in 2002 (Hallegraeff  
105 et al., 2019). Finally, in 2010 the organism appeared to have moved into the Southern Ocean  
106 for the first time (240 km south of Tasmania), raising concerns about grazing impacts on  
107 iconic krill-based food webs (McLeod et al., 2012).

108 More seriously, starting in 2012, the Tasmanian seafood industry experienced industry  
109 closures affecting bivalves, abalone, rock lobster, and public health warnings associated with  
110 Paralytic Shellfish Poisoning (up to 150 mg STX eq./kg) during winter-spring blooms of the  
111 cold-water dinoflagellate *Alexandrium catenella* (Condie et al., 2019). The morphologically  
112 identical but genetically distinct species *A. australiense* and *A. pacificum* (Bolch and  
113 DeSalas, 2007) were known from Tasmanian waters, but the presence of *A. catenella*  
114 (= *Alexandrium tamarense* Group 1; John et al., 2014), had never been previously detected.  
115 Tasmanian cultured populations are known to possess a unique microsatellite DNA signature  
116 different from other global populations, arguing that *A. catenella* has been present prior to  
117 European settlement in 1788 - 1803 and thus represents an endemic cryptic population  
118 stimulated by changing environmental conditions, such as increasing winter water column  
119 stratification (Trainer et al., 2019). At least five cases of non-fatal human paralytic shellfish

120 poisonings (one from *G. catenatum* and four from *A. catenella*) have been formally reported  
121 from Tasmania in the past 10 - 20 years, but it is unclear whether seafood poisonings may  
122 have occurred throughout longer-term (thousands of years) Tasmanian history (Jones, 1978).

123 To gain insights into long-term dynamics of harmful dinoflagellate species, their introduction  
124 into, and disappearance and reappearance in a region, marine sediment archives are a  
125 significant resource. After phytoplankton (including dinoflagellates) die or form resting  
126 stages/cysts following unfavourable conditions, they sink to the seafloor where they  
127 accumulate in layers, so that over time their fossil assemblages form a geological record of  
128 past presence and abundance. However, such microfossil assemblages can only provide part  
129 of the picture, as only the most robust species make it to the seafloor, and soft-bodied species  
130 are missing entirely from the sediment record. For example, While *Gymnodinium catenatum*  
131 produces cysts that fossilize (Anderson et al., 1988), the cysts of *Alexandrium catenella* have  
132 only limited durability in the sediment record (Head et al., 2006), and *Noctiluca* does not  
133 produce a cyst at all. Additionally, individual species of varying toxicity within the *A.*  
134 *tamarensis* species complex cannot be distinguished based on either planktonic cell or cyst  
135 morphology.

136 Recently, sedimentary ancient DNA (*sedaDNA*) analyses have been increasingly used as a  
137 tool to characterise past marine ecosystems from seafloor sediments over geological  
138 timescales. These novel *sedaDNA* analyses offer great potential to overcome the hurdle of  
139 accessing information on less-well preserved species, and gain insights into paleo-  
140 communities across all domains of life, including, phyto- and zooplankton (Armbrecht,  
141 2020). Indeed, preliminary DNA analyses on seafloor surface sediments collected near Maria  
142 Island (Spring Bay), Tasmania, first pointed to the possibility of retrieving ancient DNA  
143 preserved from all three HAB species in this region (Shaw et al., 2019). Since then, *sedaDNA*  
144 extraction techniques and bioinformatic analyses have been refined and optimized to detect,  
145 isolate and analyse the minuscule amounts of eukaryote *sedaDNA* preserved in marine  
146 sediments (Armbrecht et al., 2020, 2021). Particularly promising is the application of  
147 hybridization capture techniques to *sedaDNA*, where short RNA probes (“baits”) capture  
148 complementary DNA fragments in a DNA extract (Horn et al., 2012), an approach enabling  
149 the study of specific genes and/or organisms of interest. This ‘bait’ approach, recently applied  
150 to capture marine eukaryote *sedaDNA* (Armbrecht et al., 2021), seems highly suitable to the  
151 detailed study of past dinoflagellate dynamics and blooms of both cyst forming and non-cyst  
152 forming species.

153 We here combined palynological and *sedaDNA* techniques (including hybridization capture)  
154 to resolve the dynamics of the three HAB species *Alexandrium catenella*, *Gymnodinium*  
155 *catenatum* and *Noctiluca scintillans* over the past ~9,000 years. Our aim was to address the  
156 following questions: (1) Is there evidence from the sediment record that these three HAB  
157 species are endemic to eastern Tasmania? (2) Has their abundance changed significantly over  
158 that period? (3) What are the characteristics (*e.g.*, DNA damage and fragment size) of  
159 *Alexandrium*, *Gymnodinium* and *Noctiluca* *sedaDNA* preserved in coastal marine sediments  
160 off Eastern Tasmania, and how do these characteristics influence the predicted maximum

161 timescales of harmful dinoflagellate *sed*aDNA preservation and detection at this coring  
162 location?

163

## 164 **2 Materials and Methods**

### 165 *2.1 Sediment Core Collection and Preparation*

166 An approximately 3 m long marine sediment core (gravity core, designated ‘GC2S1’) was  
167 collected in May 2018 during *RV Investigator* voyage IN2018\_T02 in 104 m water depth  
168 close to the continental shelf edge, east of Maria Island, Tasmania (Site 1; 148.240 °E; 42.845  
169 °S) (Fig. 1). Since gravity corers can disturb the sediment surface, a shorter (12 cm) parallel  
170 core was obtained at the same site using a KC Denmark Multi-Corer (designated ‘MCS1-T6’,  
171 where ‘T6’ refers to ‘Tube 6’ of the multi-corer). A 35 cm long multi-core from within  
172 Mercury Passage, west of Maria Island (Site 3; 42.550 °S, 148.014 °E) in a water depth of 68  
173 m was also obtained (designated ‘MCS3-T2’). All cores were immediately capped, sealed,  
174 labelled and transported in their original PVC coring tubes to the Australian Nuclear Science  
175 and Technology Organisation (ANSTO), Lucas Heights, Australia, where they were kept at 4  
176 °C. GC2S, MCS1-T6, and MCS3-T6 were opened, split, scanned (using a multi-function core  
177 scanning instrument (ITRAX) with X-ray fluorescence (XRF), radiographic X-ray, optical  
178 imaging and magnetic susceptibility measurements), and subsampled for palynological and  
179 *sed*aDNA analyses in October 2018. To minimise contamination during core splitting and  
180 sampling, we wiped working benches, washed cutting knives with 3% bleach and 70%  
181 ethanol, changed gloves immediately when contaminated with sediment, and wore  
182 appropriate PPE at all times (gloves, facemask, hairnet, disposable gown). Sampling of  
183 GC2S1 was conducted by first removing the outer ~1 cm of the working core-half and then  
184 taking subsamples by pressing sterile 15 mL centrifuge tubes ~3 cm into the sediment at 5 cm  
185 intervals (working from bottom to the top of the core at each step). Sampling of MCS1-T6  
186 was conducted as for GC2S1 except at finer intervals of 2 cm. Mercury Passage multicore  
187 (MCS3-T2) sampling was conducted at 2 cm depth intervals in the top 8 cm and at 5 cm  
188 intervals below. All palynology and *sed*aDNA samples were immediately stored at 4 and -20  
189 °C, respectively. Hereafter, we refer to sediment depths as 0 cm, 2 cm, etc., however, it  
190 should be noted that, due to centrifuge tubes in which samples were collected being ~1.5 cm  
191 diameter, this actually describes a sample depth interval of 0 - 1.5 cm, 2 – 3.5 cm, etc.,  
192 respectively.

193

### 194 *2.2 Sediment dating*

195 ITRAX scanning, XRF, radiographic X-ray, optical imaging and magnetic susceptibility  
196 measurements confirmed excellent undisturbed preservation of the cores. Dating of MCS3-  
197 T2 and MCS1-T6 was based on <sup>210</sup>Pb (8 and 6 depths, respectively) and dating of and GC2S1  
198 on both <sup>210</sup>Pb (7 depths) and <sup>14</sup>C (3 depths) measurements. A Bayesian age-depth model was

199 constructed for each site based on these  $^{210}\text{Pb}$  and  $^{14}\text{C}$  measurements using the rbacon  
200 (Blaauw et al., 2019) software in on the R platform (R Core Team, 2013) with the SHCal20  
201 curve for radiocarbon age calibration (Hogg et al., 2020). Details on the construction of the  
202 age-depth model is provided within the Supplementary Material (Supplementary Material  
203 Fig. 1 and Table 1).  
204

### 205 2.3 *Palynological treatment and microscopy*

206 Micropaleontological dinocyst slide preparation involved disaggregation in hydrofluoric acid  
207 (HF), density separation in a  $\text{ZnBr}_2$  solution (specific gravity 2.1), sieving on 8  $\mu\text{m}$  filters,  
208 and mounting in permanent mounting medium (Eukitt). One tablet of *Lycopodium clavatum*  
209 spores (Department of Geology, Lund University, Sweden, batch no. 938934, mean spores  
210 per tablet =  $10,679 \pm 426$ ) was added to each sample to be used as a “tracer” as per Stockmarr  
211 (1971). Microscopy slides were counted for dinoflagellate cysts and *Lycopodium* spores,  
212 and cysts per  $\text{g}^{-1}$  of sediment calculated by relating cysts to spore counts. Slides were  
213 analysed using a Nikon Eclipse Ci light microscope with multiple transects viewed at 200 $\times$   
214 magnification until a cyst count >100 was achieved. To improve recognition and counting of  
215 *Alexandrium* cysts, we applied primulin fluorochrome staining as developed by Yamaguchi et  
216 al. (1995) to all samples from the inshore (MCS3-T2) and shelf edge (MCS1-T6 and GC2S1)  
217 cores. While the staining protocol as originally prescribed applies to aqueous samples, both  
218 the aqueous and ethanol residues left over after palynological treatment were successfully  
219 stained. Taxonomy of the cysts was also aided by examining selected examples using a  
220 Hitachi SU-70 Scanning Electron Microscope (SEM). Nikon NIS-Elements software was  
221 used to capture light and fluorescence images during microscopy. Images were arranged for  
222 plate presentation using Microsoft Publisher. The paleontological software package TiliaIT  
223 was used for graphing of cyst profile data. A ratio was drawn between the number of  
224 dinocysts categorized as either heterotroph or autotroph per sample (Supplementary Material  
225 Table 2).  
226

### 227 2.4 *Sedimentary ancient (sedaDNA) extractions, hybridization capture and sequencing* 228 *library preparations*

229 Extractions of *sedaDNA* took place at ACAD's ultraclean ancient (GC2S1) and forensic  
230 (MCS1-T6, MCS3-T2) facilities following the recommended ancient DNA decontamination  
231 standards (Willerslev and Cooper, 2005). The extraction technique followed the new  
232 ‘combined’ protocol specifically developed to isolate marine eukaryote *sedaDNA* described  
233 in Armbrrecht et al. (2020). This method combines a gentle EDTA incubation step to isolate  
234 fragile DNA along with a bead-beating step to extract intracellular DNA from robust spores  
235 and cyst, and further retains very small ( $\geq 27$  base pairs, bp) DNA fragments characteristic of  
236 ancient DNA by using in-solution silica binding and magnetic beads to size-select DNA  
237 fragments under 500 bp. *sedaDNA* extracts and metagenomic shotgun libraries were prepared  
238 from 42 sediment samples (MCS3-T2 and GC2S1) and 7 extraction blank controls following  
239 Armbrrecht et al. (2021). Sequencing was undertaken using an Illumina NextSeq sequencing

240 platform (2 x 75 bp cycle) at the Australian Cancer Research Foundation Cancer Genomics  
241 Facility & Centre for Cancer Biology, Adelaide, Australia, and at the Garvan Institute of  
242 Medical Research, KCCG Sequencing Laboratory Kinghorn Centre for Clinical Genomics,  
243 Darlinghurst, Australia.

244

245 In order to maximise the yield of *seda*DNA from our target dinoflagellates, we applied a  
246 hybridization-capture technique. This technique uses short RNA probes ('baits') that are  
247 designed to be complementary to any DNA sequences of interest in the DNA extract to  
248 capture and enrich these target sequences (Horn et al., 2012). In collaboration with Arbor  
249 Biosciences, USA, a 'bait set' was developed that targeted the harmful dinoflagellates  
250 *Alexandrium* groups I – IV, *Gymnodinium catenatum* and *Noctiluca scintillans*  
251 ('HABbaits1'). Details on HABbaits1 design and application to 27 selected marine *seda*DNA  
252 extracts including protocol optimizations are provided in Armbrrecht et al. (2021). A final  
253 pool of multiplexed sequencing libraries prepared from HABbaits1 was submitted for  
254 Illumina sequencing (HiSeq XTen, 2 x 150 bp cycle) to the KCCG, Darlinghurst, Australia.

255

256 Bioinformatic processing of the sequencing data (shotgun and hybridizations) followed  
257 established protocols previously described in detail in Armbrrecht et al. (2020), with software  
258 versions and analytical parameters as described in Armbrrecht et al. (2021). After filtering  
259 (low-complexity and duplicate reads removed), we processed each dataset (*a*) without  
260 standardising (i.e., non-rarefying) to retain the maximum number of reads, which is crucial  
261 for *seda*DNA damage analysis (see below), and (*b*) with standardising by subsampling (i.e.,  
262 rarefying) each dataset to the lowest number of reads detected in a sample, i.e., 2.2 million  
263 (Mio) and 0.2 Mio for the shotgun and HABbaits1 data, respectively (using seqtk version  
264 1.2). The latter was done to be able to assess our data semi-quantitatively. Non-rarefied and  
265 rarefied data resulting from (*a*) and (*b*), respectively, were then continued to be processed in  
266 parallel.

267

268 After quality control (FastQC v.0.11.4, MultiQC v1.8), we used the NCBI Nucleotide  
269 database (<ftp://ftp.ncbi.nlm.nih.gov/blast/db/FASTA/nt.gz>, downloaded November 2019) as  
270 the reference database to build a MALT index (Step 3) and aligned our sequences using  
271 MALT (version 0.4.0; semiglobal alignment) (Herbig et al., 2016). We converted all resulting  
272 .blastn to .rma6 files using the Blast2RMA tool in MEGAN (version 6\_18\_9, Huson et al.,  
273 2016). Subtractive filtering (i.e., subtracting reads for species identified in EBCs from  
274 samples) was conducted separately for the shotgun and HABbaits1 data (see Armbrrecht et al.,  
275 2021 Supplementary Material, for a comprehensive list of eukaryote contaminants), however,  
276 no Dinophyceae taxa were detected in EBCs. For each dataset (shotgun and HABbaits1), we  
277 exported the read counts for all Dinophyceae nodes (from MEGAN6 v. 18.10) for  
278 downstream analyses. Additionally, we exported read-length data (non-rarefied shotgun and  
279 HABbaits1 data) for Dinophyceae and the genera *Gymnodinium*, *Alexandrium* and *Noctiluca*  
280 (separately for each coring site) to assess whether cyst-formers preserve better than non-cyst  
281 formers (assumedly reflected in longer vs. shorter read lengths, respectively).

282

283 To test *sedaDNA* damage, we ran the ‘MALTEExtract’ and ‘Postprocessing’ tools of the  
284 HOPS v0.33-2 pipeline (Hübler et al., 2020) using the same configurations as in Armbrecht  
285 et al. (2021; taxalist ‘b’, which included our three target dinoflagellate species) on shotgun  
286 and HABbaits1 *sedaDNA* data (non-rarefied, as retaining a high number of reads is critical  
287 for this step). Authenticity of the Maria Island *sedaDNA* data has been supported previously  
288 through an increasing proportion of eukaryote *sedaDNA* damage with subseafloor depth in  
289 both shotgun and HABbaits1 datasets (Armbrecht et al., 2021). Here we focus on *sedaDNA*  
290 damage analysis of the harmful dinoflagellate taxa *Alexandrium catenella*, *A. fundyense* and  
291 *A. tamarensense* Group1 (hereafter grouped as *A. catenella* as these have recently all been  
292 defined as the same species, John et al., 2014), *Gymnodinium catenatum* and *Noctiluca*  
293 *scintillans*. To do so, we analysed the MaltExtract output, *i.e.*, reads categorized as ancient  
294 (showing damage) or default (passing stringent filtering criteria but not showing damage) for  
295 these three taxa (Hübler et al., 2020), and, based on the latter, we determined the proportion  
296 of *sedaDNA* damage per species. Also, *sedaDNA* damage profiles were generated for these  
297 three taxa using MaltExtract Interactive Plotting Application (MEx-IPA, by J. Fellows Yates;  
298 <https://github.com/jfy133/MEx-IPA>).  
299

### 300 **3 Results**

#### 301 *3.1 Dinoflagellate Cysts*

##### 302 *3.1.1 Total Dinocyst abundance*

303 Total dinocyst abundance in the inshore core MCS3-T2 (35 cm long) was highest at the  
304 surface (3,228 cysts g<sup>-1</sup> dry sediment at 5 - 6.5 cmbsf) and decreased steadily with depth  
305 (until ~30 cmbsf). A similar surface peak was observed for *Alexandrium*, *Protoceratium*  
306 *reticulatum*, *Protoperidinium* and *Spiniferites* taxa along with a second peak at the bottom of  
307 the core (~34 cmbsf) was only observed for the latter three taxonomic groups. At the offshore  
308 site, in MCS1-T6 (12 cm long), total cyst numbers increased with depth (5,504 g<sup>-1</sup> dry  
309 sediment). In GC2S1, cyst abundance was greatest in younger sediments (3,090 g<sup>-1</sup> dry  
310 sediment at 41 - 42.5 cmbsf). Summarising cyst composition as the ratio of heterotroph  
311 (mostly *Protoperidinium*) to autotroph dinoflagellate cysts (mostly *Protoceratium*,  
312 *Spiniferites*), heterotrophs contributed 40% of cysts inshore (MCS3-T2), 38% at the surface  
313 sediment at shelf edge (MCS1-T6) but decreasing to 14% at the bottom of MCS1-T6.  
314 Throughout the deeper section of the GC2S1 core the heterotroph to autotroph ratio was  
315 comparatively constant. In GC2S1 the contribution by *Protoceratium* decreased from 62% of  
316 total cysts at the surface down to 16% at the bottom at ~9,000 years old, with *Spiniferites*  
317 taking over dominance (Fig. 2).  
318



### 319 3.1.2 *Dinocyst species composition*

320 A total of 4,279 dinoflagellate cysts comprising 32 species (28 in GC2S1, 6 in MCS1-T6, and  
321 10 in MCS3-T2) were examined from 44 sediment samples. Most abundant offshore were the  
322 cysts of *Protoceratium reticulatum* (46 - 63% of total cysts; Fig. 3A-C), while the most  
323 abundant inshore were *Spiniferites* (including *S. bulloideus*, *S. hyperacanthus*, *S.*  
324 *membranaceus*, *S. mirabilis*, *S. pachydermis*, *S. ramosus*; combined 42% of total cysts; Fig.  
325 3D-H) and *Protoperidinium* (*P. avellana*, *P. conicum*, *P. minutum*, *P. oblongum*, *P.*  
326 *subinermis*, *P. shanghaiense*, unidentified peridinoid “round browns”; 39% of total cysts;  
327 Fig. 3M-O). Rarer cyst species included *Impagidinium aculeatum*, *I. paradoxum*, *I. patulum*,  
328 *I. plicatum*, *I. cf. striatum*, *I. sphaericum* (Fig. 3I) and *Nematosphaeropsis labyrinthus* (Fig.  
329 3J) all offshore only) and *Polykrikos schwartzii* (inshore only). Typical warm-water cyst taxa  
330 such as *Lingulodinium machaerophorum* and *Tuberculodinium vancampoea* were not  
331 detected.

332

333 The microreticulate cyst of *Gymnodinium catenatum* (Fig. 3S) was only detected inshore and  
334 in very low concentrations (9 cysts in total), present in the upper part of the MCS1-T2 core  
335 with a peak of 113 cysts g<sup>-1</sup> dry weight at 12 – 13.5 cmbsf (centimetre below sediment  
336 surface) and the oldest specimens (~50 years) observed at 16 cmbsf. Low concentrations of  
337 the microreticulate cysts of the smaller *Gymnodinium microreticulatum* were also detected  
338 (Fig. 3T; 3 cysts seen only, 1 each at 0 - 1.5 cmbsf, 15 – 16.5 cmbsf, and 30 – 31.5 cmbsf;  
339 Bolch and Reynolds, 2002). Detection of the bean-shaped cysts of the genus *Alexandrium*  
340 was enhanced by the use of primulin fluorescence microscopy Figs. 3 P-R). The MCS3-T2  
341 inshore core contained *Alexandrium* cysts in 50% of sampled segments using standard light  
342 microscopy (37 cysts seen) but in 80% of samples when utilising primulin staining. Highest  
343 concentrations of 364 cysts g<sup>-1</sup> dry sediment occurred in the surface sediments of MCS3-T2  
344 and with cysts detected down to 35 cm depth (145 years old). Low concentrations of  
345 comparable cysts (23 cysts seen in total; 4 cysts g<sup>-1</sup> dry sediment) were observed in the  
346 offshore GC2S1 core down to 264 cmbsf (~9,000 years old). However, none of the offshore  
347 *Alexandrium*-like cysts responded to primulin staining. Staining enhanced visibility of the  
348 archeopyle in translucent cyst taxa such as *Protoperidinium shanghaiense* (Fig. 3L) and  
349 *Spiniferites* spp. or aided detection where cysts were obscured by detrital material.

350

## 351 3.2 *Sedimentary ancient DNA*

### 352 3.2.1 *Representation of Dinophyceae in shotgun data*

353 We retrieved a total of 824,503 filtered sequences across the 42 shotgun samples, 149,892 of  
354 which were assigned to Eukaryota (18%), and 529 to Dinophyceae (0.06%). Harmful  
355 dinoflagellate taxa were detected at low abundance (19 *Alexandrium* spp., 13 *Gymnodinium*  
356 spp., and no *Noctiluca* sequences; Supplementary Material Fig. 2). Normalising the Shotgun  
357 data (i.e., rarefying/subsampling to 2.2 Mio reads per sample) reduced the number of reads  
358 assigned to Dinophyceae to a total of 148. As expected, rarefaction led to the detection of  
359 less reads of harmful Dinophyceae taxa, with *Gymnodinium* only resolved to genus level in

360 MCS3-T2 and GC2S1, and only one *A. catenella* sequence detected in MCS3-T2  
361 (Supplementary Material Fig. 3). In GC2S1 the read numbers showed some cyclicity  
362 throughout the core, suggesting relatively high Dinophyceae abundance (up to 10 reads per  
363 sample) between 189 and 240.5 cmbsf, and 50 - 56.5 cmbsf (Supplementary Material Fig. 3).  
364 Due to the scarcity of Dinophyceae reads in the shotgun data, we focus on presenting  
365 HABbaits1 results below.  
366

### 367 3.2.2 Representation of Dinophyceae in HABbaits1

368 By applying HABbaits1 to our 27 selected *seadaDNA* extracts, a total of 32,075 sequences  
369 were retrieved and assigned to Dinophyceae, respectively. After rarefying to 0.2 Mio reads  
370 for HABbaits1, these totals were reduced to 4,456 Dinophyceae sequences. HABbaits1  
371 provided a total of 186, 267, and 28 sequences assigned to *Alexandrium* spp., *Gymnodinium*  
372 spp., and *Noctiluca scintillans* (Fig. 4).  
373

374 HABbaits1 showed that *Alexandrium* were most abundant at MCS3-T2, with the maximum  
375 number of reads (107 sequences) found in MCS3-T2 12 - 13.5 cmbsf (Fig. 4A). *A. tamarensense*  
376 (not further classified) was identified at this depth (2 reads) as well as in the surface sample  
377 MCS2-T2 2 - 3.5 cmbsf. *A. catenella* was identified at MCS3-T2 6 - 7.5 cm (1 read). At  
378 GC2S1, *Alexandrium* spp. were in low abundance (<5 reads per sample), with *A. tamarensense*  
379 being detected at 139 - 14.5 cmbsf (1 read, Fig. 4B). *A. catenella* were identified in GC2S1 at  
380 75 - 76.5 (1 read) and 189 - 190.5 cmbsf (2 reads) (Fig. 4B).  
381

382 A number of reads were assigned to *G. catenatum* in both the inshore and offshore core,  
383 however, given the recent introduction hypothesis, and observations that Tasmanian  
384 populations are generally estuarine-bound (McMinn et al., 1998), further inspection of these  
385 sequences was undertaken. Supplementary comparative analysis of these sequences revealed  
386 all fell within the microreticulate-group of five *G. catenatum*-like species, and the majority  
387 within 1 - 3 bp of *G. catenatum* large subunit (LSU) ribosomal rRNA genes reference  
388 sequence DQ785882 (see Supplementary Material Table 3, Supplementary Material Fig.  
389 4,5,6,7). The *G. catenatum*-like species was identified in the surface sample of MCS3-T2 2 -  
390 3.5 cm, alongside *G. microreticulatum* (1 read each, Fig. 4C). At GC2S1, the *G. catenatum*-  
391 like species appeared sporadically in low abundance (1 read) in the upper section of GC2S1  
392 (above 75 - 76.5 cmbsf), while being slightly more abundant ( $\leq 6$  reads) in the lower section  
393 of the core (below 169 - 170.5 cmbsf; Fig. 4D).  
394

395 The application of HABbaits1 also allowed the identification of *N. scintillans* in the Maria  
396 Island sediment cores. *N. scintillans* occurred primarily in the upper section of MCS3-T2  
397 (above 15 cmbsf), reaching its maximum abundance (9 - 10 sequences) at 6 - 7.5 and 12 -  
398 13.5 cmbsf (Fig. 4E). This species was able to be detected in the two top samples at GC2S1  
399 (1 sequence each, Fig. 4F). It should be noted, however, that while a low number of *G.*  
400 *catenatum* and *N. scintillans* sequences were detected in our deepest sample (Fig. 4D,F), this

401 observation should be treated with caution due to the possibility of seawater contamination of  
402 this very bottom sample during core retrieval.  
403

### 404 3.2.3 *sedaDNA damage analysis and authentication*

405 As the shotgun dataset recovered relatively few reads from the targeted dinoflagellate taxa,  
406 we focused on analysing damage patterns in HABbaits1. HABbaits1 (non-rarefied) provided  
407 0, 4, and 1 ancient reads for *A. catenella*, *G. catenatum*-like, and *N. scintillans* at site MCS3-  
408 T2, respectively, and 13, 95, and 11 ancient reads for *A. catenella*, *G. catenatum*-like, and *N.*  
409 *scintillans* at site GC2S1, respectively (Table 1). A comparatively high number of reads  
410 passed the default filtering criteria in HOPS (Table 1). Expressed in percentages, 0% and  
411 41% of the *A. catenella* reads were classified as ancient (*i.e.*, showed clear signs of DNA  
412 damage) in MCS3-T2 and GC2S1, respectively. For *G. catenatum*-like, 4% and 27% of reads  
413 were classified as ancient in MCS3-T2 and GC2S1, respectively, and for *N. scintillans*, 0.5%  
414 and 18% were classified as ancient (Table 1). As such, reads assigned to the three target  
415 dinoflagellates showed much higher *sedaDNA* damage at the offshore site GC2S1 relative to  
416 the inshore site MCS3-T2. Due to the scarcity of reads categorized as ancient, few *sedaDNA*  
417 profiles could be generated, especially for the inshore site MCS3-T2, however, all profiles  
418 generated for the three target dinoflagellates are included in Supplementary Material Fig. 8  
419 for completeness.  
420

### 421 3.2.4 *Sequence length analysis of cyst vs. non-cyst formers*

422 Slight differences in *Alexandrium*, *Gymnodinium*, and *Noctiluca* read lengths were found  
423 when compared to overall Dinophyceae read lengths in the shotgun and HABbaits1 datasets.  
424 However, due to very low read numbers recovered by the shotgun data, and high standard  
425 deviations of average fragment lengths per taxon, we do not consider these statistically  
426 robust, thus provide this data with the Supplementary Material (Supplementary Material Fig.  
427 9).  
428

## 429 4 Discussion

430 This study presents the first marine sediment core analysis of dinoflagellate cyst assemblages  
431 off the Tasmanian east coast and defines a clear demarcation between long-term  
432 dinoflagellate cyst species in subtropical New South Wales waters (McMinn, 1992) and  
433 temperate Tasmanian waters. Typical warm-water cyst taxa such as *Lingulodinium*  
434 *machaerophorum* and *Tuberculodinium vancampoea*, common in New South Wales, were  
435 notably absent off Maria Island, and reflect limitations in the southward penetration of the  
436 East Australian Current into Tasmanian shelf waters throughout the past ~9,000 years. The  
437 most prominent inshore cyst taxa were *Spiniferites* spp. whilst cysts of *Protoceratium*  
438 *reticulatum* dominated offshore. *Protoperidinium* displayed episodic peaks inshore, but were  
439 more consistently present offshore. Through a combined approach of palynology and

440 *sedaDNA* analysis, this study provides the first evidence of the presence and changing  
441 abundance of the three harmful dinoflagellates *A. catenella*, *G. catenatum*-like, and the soft-  
442 bodied non-cyst-former, *N. scintillans* in Australian waters covering a ~9,000-year time-  
443 period.  
444

#### 445 4.1 *HAB species presence around Maria Island, Tasmania, over the last 9,000 years*

##### 446 *Alexandrium*

447 Both palynology and *sedaDNA* showed that the *A. tamarense* species complex has been  
448 present inshore and offshore of Maria Island since ~145 and at least ~9,000 years,  
449 respectively. *Alexandrium* can be a prolific cyst producer (by approximately 40% of  
450 vegetative cells; Anderson et al., 2014). Inshore, *Alexandrium* cysts could be clearly  
451 identified via primulin staining, while surprisingly offshore none of the *Alexandrium*-like  
452 cysts responded to the same staining. This may suggest degradation of the cellulose cyst wall  
453 at sediment ages exceeding ~145 years. Although we consider the following less likely due to  
454 detailed inspection by microscopy, the lack of staining could also mean that these were non-  
455 *Alexandrium* cysts (Yamaguchi et al., 1995). However, *sedaDNA* (HABbaits1) implied that  
456 the genus *Alexandrium* became abundant in inshore waters in recent years (~15 years ago to  
457 present), and also offshore at around 2,300, ~6,000, and prior to ~7,200 years ago. The  
458 offshore *Alexandrium* *sedaDNA* peak at 2,300 years ago matches a putative cyst peak  
459 (supporting the identification of these cysts as *Alexandrium* despite non-staining). *sedaDNA*  
460 (HABbaits1) identified *Alexandrium* spp. at nearly all sampled depths of GC2S1, including  
461 the toxic *A. catenella* at ~3,500 and ~7,200 years ago (Fig. 4B). This observation confirms  
462 the previous suggestion that this species has been endemic in the Tasmanian region before  
463 being stimulated by climate changed-induced environmental conditions (Condie et al., 2019).  
464 The HABbaits1 enriched *sedaDNA* was unable to discriminate between *Alexandrium*  
465 genotypes 1 (*catenella*), 4 (*pacificum*) and 5 (*australiense*) through the core because the  
466 fragments retrieved mapped to somewhat more conserved gene regions including the rRNA  
467 gene. Increased starting material and HABbaits1 enrichment, combined with increased  
468 sequencing depth would provide higher probability of recovering *sedaDNA* fragments from  
469 the most informative regions of the rRNA genes such the D1-D2 regions of the LSU, and the  
470 rRNA ITS-regions successfully targeted in these species for detection using qPCR (e.g.,  
471 Ruvindy et al., 2018).

##### 472 *Gymnodinium*

473 Both palynology and *sedaDNA* identified *G. catenatum* at the inshore site at ~15 (*sedaDNA*)  
474 and ~30 years ago (palynology) and, to a lesser degree in recent sediments ~2 years ago  
475 (palynology and HABbaits1). A presence 30 years ago (~1990) corresponds to a period when  
476 *G. catenatum* represented approx. 9% of resting cysts in surface sediments of Spring Bay  
477 (Bolch and Hallegraeff 1990). No *G. catenatum* cysts were detected in the offshore core  
478 using palynology, but it is noted that *G. catenatum* is a very poor cyst producer (1 - 2% of  
479 vegetative cells; Blackburn et al., 2001). *sedaDNA* identified *G. catenatum*-like sequences  
480 sporadically throughout the entire length of GC2S1, with slightly higher representation at  
481 greater depths (~6,700 - 9,000 years ago). This was unexpected as, based on duplicate

482 sediment cyst core studies in the neighbouring Huon River (100 km distant), *G. catenatum* is  
483 thought to have been introduced to Tasmania via ship's ballast water in the 1970s (McMinn  
484 et al., 1998).

485

486 The reliability of species assignments of *Gymnodinium* spp. from rRNA genes (internally  
487 transcribed spacer (ITS), small subunit (SSU) and large subunit (LSU) rRNA) using a  
488 synthetic dataset showed that 18S rRNA (SSU) sequences of *G. catenatum* and *G.*  
489 *microreticulatum* can only be confidently assigned to order-level (e.g., Gymnodiniales),  
490 especially when sequences are short as were our *sedaDNA* sequences (~56 bp on average in  
491 the shotgun data) (see Supplementary Material Table 3, Supplementary Material Fig. 4).  
492 However, in this study we recovered LSU rRNA gene sequences, which were (in contrast to  
493 SSU) assignable below genus level. All *G. catenatum*-related *sedaDNA* LSU-rRNA gene  
494 sequences (44 – 129 bp) mapped downstream of the LSU D1-D3 region and were confirmed  
495 to be most similar to *G. catenatum* but not an exact match (Supplementary Material Fig.  
496 5,6,7). The latter was determined by mapping the *sedaDNA* sequences to publicly available  
497 *Gymnodinium* LSU reference sequences (which has low taxon coverage as only three  
498 reference sequences are available, *G. catenatum*, *G. aureolum*, *G. impudicum*), as well as to  
499 newly, in-house generated sequences of the LSU D3-D10 region (~2,000 bp) of *G.*  
500 *microreticulatum* and *G. nolleri* (Supplementary Material Fig. 5,6,7). The *G. catenatum* LSU  
501 reference sequence DQ785882 which the *sedaDNA* fragments matched most closely is from  
502 a cultured Korean *G. catenatum* isolate, and the small (1 – 3 bp) differences may reflect  
503 sequence variation between Australian and other populations (e.g., Bolch and De Salas, 2007)  
504 or perhaps the existence of related but as yet undescribed or unreported cryptic species.  
505 Sequence variation among dinoflagellates across the D3-D10 region is also considerably  
506 lower than the hypervariable regions between D1 and D2. When combined with the low  
507 taxon coverage, we cannot conclusively determine whether these sequences represent *G.*  
508 *catenatum* or another related microreticulate group species. A recent introduction via ballast  
509 water, superimposed upon an indigenous cryptic population remains a possible interpretation.  
510 Additional studies with increased sample and/or sequencing depth and improved coverage of  
511 full length rRNA genes from gymnodinoid taxa are necessary more firmly establish the most  
512 probable explanation for our data.

513 *Noctiluca*

514 HABbaits1 revealed the presence of *N. scintillans* inshore of Maria Island over the last ~30  
515 years, as well as traces of this dinoflagellate in shallow sediments offshore (0 – 1.5 and 5 –  
516 6.5 cmbsf; <100 years old). Inshore, the highest abundances of *N. scintillans* were detected in  
517 relatively recent sediments (6 – 7.5 and 12 – 13.5 cmbsf), indicating bloom phases of this  
518 species occurred within the last 7 – 15 years, corroborating the observational record. *N.*  
519 *scintillans* was first detected in Tasmania in 1994 and thought to be driven by increased  
520 southward extension of the East Australian Current. Since then, blooms of this dinoflagellate  
521 have increased in both frequency and intensity (Hallegraeff et al., 2019). To our knowledge,  
522 this is the first time that *N. scintillans* *sedaDNA* has been reported from a coastal ecosystem  
523 into which it has been introduced, demonstrating the sensitivity of the HABbaits1 approach

524 for detecting plankton community change of fragile non-fossilizing species from the marine  
525 sediment record. *N. scintillans* was identified in the deepest sample at GC2S1, however, our  
526 HOPS analysis showed that *sedaDNA* damage in this sample was very low (1 ancient vs. 32  
527 default reads in the non-subsampled HABbaits1 data), so we cannot exclude the possibility  
528 these are modern sequences originating from seawater contamination during coring.  
529

#### 530 4.2 Reconstructing paleo-blooms

531 The abundance of *Alexandrium*, *Gymnodinium*, and *Noctiluca* through time were assessed  
532 using subsampled shotgun and HABbaits1 datasets. The shotgun data showed variations in  
533 the total abundance of Dinophyceae at the offshore site, and periods of increased abundance  
534 at ~2,300 and ~7,200 – 9,000 years ago largely contributed by increased *Gymnodinium* spp.  
535 (Supplementary Material Fig. 3). However, differences in gene copy number amongst species  
536 can influence their over-/under-representation in *sedaDNA* therefore the data should be  
537 viewed as semi-quantitative. To investigate whether individual HAB-species might have  
538 undergone bloom-phases, HABbaits1 data was examined separately for each of the three  
539 dinoflagellates of interest. By doing so, it was determined that high abundances of  
540 *Alexandrium* spp. at ~15 years ago, indicate a bloom phase (inshore). *G. catenatum*-like read  
541 numbers were elevated between ~ 6,700 – 9,000 years ago, but as indicated above this  
542 species assignment is unclear. Blooming of *N. scintillans* in recent years, particularly inshore,  
543 is supported through elevated abundances of reads of this species between 17 - 15 years ago.  
544 Similar ‘appear and disappear’ HAB patterns have started to emerge from both palynological  
545 and sediment environmental DNA studies in the Northern Hemisphere. For example,  
546 *Gymnodinium catenatum* first became a problem in Spain and Portugal in 1976, but cyst  
547 records date back to the late 1800s, 75 years before the first human PSP poisonings occurred  
548 (Ribeiro et al., 2012). *Alexandrium minutum* has been associated with PSP problems in the  
549 Bay of Brest, France only since 2012, but environmental DNA studies of sediment cores  
550 demonstrated its presence in the area since the late 1800s (Klouch et al., 2018).  
551

#### 552 4.3 Characteristics of harmful dinoflagellate *sedaDNA* preserved in coastal marine 553 sediments off Eastern Tasmania and implications for long-term preservation

554 Our *sedaDNA* approach allowed the assessment of authenticity for sequences recovered for  
555 *A. catenella*, *G. catenatum*-like, and *N. scintillans*. The % *sedaDNA* damage was low for  
556 sequences belonging to the three target taxa at MCS3-T2 (up to 4% for *G. catenatum*-like),  
557 however, this was expected and in line with the finding that eukaryote *sedaDNA* damage is  
558 generally very low in the upper ~35 cm of sediment at this site (Armbrecht et al., 2021).  
559 Offshore, the increased proportion of *sedaDNA* damage observed (up to 41% for *A.*  
560 *catenella*) indicate that the *A. catenella*, *G. catenatum*-like and *N. scintillans* sequences are  
561 authentic, with the exception of the bottom-core sample where contamination by seawater  
562 cannot be ruled out.  
563

564 The advantage of combining palynological and *sedaDNA* records to investigate the long-term  
565 presence of harmful dinoflagellates becomes clear when soft-bodied, non-cyst-forming  
566 species are considered. Our *Noctiluca* *sedaDNA* evidence matches the observational records,  
567 and the reduced relative abundance offshore is consistent with *N. scintillans* blooms being  
568 predominantly coastal (Hallegraeff et al., 2019). However, the presence of *N. scintillans*  
569 *sedaDNA* in recent sediments at the offshore site confirmed that its DNA has been preserved  
570 at the seafloor after sinking through a 140 m water column. Future research into the mode of  
571 downward transport (e.g., sinking after dying, or transport inside copepod faecal pellets)  
572 might provide further insights into this new finding. While determined from relatively low  
573 number of reads (60), *N. scintillans* *sedaDNA* shows signs of damage, especially at the  
574 offshore site, indicating that the DNA of this soft-bodied dinoflagellate does not preserve  
575 well for long and may pose limitations to its analysis using *sedaDNA* records. Future  
576 investigations could target sediment cores from Sydney, where this species has been present  
577 closer to shore for longer and rate of damage of *N. scintillans* *sedaDNA* might be estimated  
578 over longer timescales.

579

580 The microfossil and *sedaDNA* data presented here both support the suggestion that *A.*  
581 *catenella* has been present in Tasmania throughout the last ~9,000 years and that recent  
582 bloom events are associated with alterations in oceanographic conditions (Condie et al.,  
583 2019). Hybridization capture *sedaDNA* confirmed the presence of *Alexandrium* offshore  
584 where unambiguous identification by microscopy was limited due to the lack of a primulin  
585 staining response by the cysts. It is noteworthy that toxic *Alexandrium catenella* blooms may  
586 have occurred around 3,500 years ago (supported in this study by *sedaDNA*), as this falls into  
587 the time period when Tasmanian aboriginals reportedly stopped (or, at least limited) to  
588 consume scaled fish (~3,000 - 4,000 BP; Jones, 1978, Taylor, 2007), however, a relationship  
589 between these two events is entirely speculative.

590

591 Detecting *G. catenatum* *sedaDNA* sequences in GC2S1 samples of up to 9,000 years in age  
592 conflicts with a well-established recent introduction hypothesis. While the *sedaDNA*  
593 fragment assignment process used in this study proved to be robust, the limited availability of  
594 gymnodinoid reference sequences covering the full-length LSU rRNA gene operon sequences  
595 means conclusive identification of the *G. catenatum*-like species in *sedaDNA* was not  
596 possible. This has two significant consequences for the use of *sedaDNA* to infer the past  
597 plankton community structures over longer timescales. First, it demonstrates the importance  
598 of closely investigating the source, characteristics, and authenticity of the typically very short  
599 *sedaDNA* fragments before drawing conclusions; second, the urgent need for more complete  
600 reference sequences for many species of interest (including *Gymnodinium*) if robust species-  
601 level resolution is anticipated.

602

## 603 **5 Conclusions**

604 Our study provides new insights into the long-term presence and prevalence cycles of three  
605 HAB species in the Tasmanian region, including preliminary clues to their blooming phases.  
606 Both palynological and *sedaDNA* analyses confirmed the presence of *Alexandrium* over  
607 thousands of years. Strikingly, *Alexandrium* cysts from inshore sediments responded to  
608 primulin fluorescence staining, but older offshore *Alexandrium* cysts did not, the significance  
609 of which is unclear. The detection of cysts of *Gymnodinium catenatum* in 50-year-old inshore  
610 sediments support the body of evidence of a ballast water introduction into Tasmania,  
611 previously postulated from shorter (25 to 80 cm long, 100 - 200-year-old) Huon River  
612 sediment cores (McMinn et al., 1998). However, the occurrence of *G. catenatum*-like  
613 *sedaDNA* throughout the offshore core suggests a possible similar long-time history  
614 (thousands of years) for a *G. catenatum* related species in Tasmanian waters, requiring  
615 further research to confirm the authenticity and identity of these sequences. From *sedaDNA*  
616 hybridization capture data we confirm that the range expansion of the non-cyst forming, soft-  
617 walled *Noctiluca* to Tasmanian waters represents an unprecedented change to this regional  
618 marine ecosystem since the 1990s. Application of similar methods to the putative range  
619 expansion of green *Noctiluca* (with green algal symbionts) into the Arabian Sea (Gomes et  
620 al., 2014) would be of considerable interest.

621

622

## 623 **Acknowledgements**

624 We are grateful to Brian Brunelle from Arbor Biosciences, USA, for his expert assistance  
625 with designing HABbaits1. We thank Oscar Estrada-Santamaria, Steve Richards, Holly  
626 Heiniger, Nicole Moore and Steve Johnson for their help and advice during extractions,  
627 library preparations, and hybridization capture. We are grateful to Raphael Eisenhofer, Vilma  
628 Pérez, Yassine Souilmi, Yichen Liu, and Ron Hübler for their help with bioinformatic  
629 analyses. We thank the Marine National Facility, the crew of RV *Investigator* voyage  
630 IN2018\_T02 and the scientific voyage team for their support during field work [2018 MNF  
631 Grant H0025318]. We thank Mr Shikder Saiful Islam (IMAS, University of Tasmania) for  
632 contributing additional rRNA gene sequence data from microreticulate *Gymnodinium* species.  
633 We thank Henk Heijnis for logistical support and his contributions to secure funding for this  
634 project. This study was funded through the Australian Research Council [ARC Discovery  
635 Project DP170102261]. AC was funded by ARC Laureate Fellowship FL140100260.

## 636 **References:**

637

638 Anderson, D.M., Jacobson, D.M., Bravo, I., Wrenn, J.H. 1988. The unique, microreticulate  
639 cyst of the naked dinoflagellate *Gymnodinium catenatum* Graham. *Journal of Phycology* 24,  
640 255-262.

641

642 Anderson, D.M., Keafer, B.A., Kleindist, J.L., McGillicuddy, D.J., Martin, J.L., Norton, K,



- 643 Pilskaln, C.H., Smith, J.L., Sherwood, C.R., Butman, B. 2014. *Alexandrium fundyense* cysts  
644 in the Gulf of Maine: long-term time series of abundance and distribution, and linkages to  
645 past and future blooms. *Deep Sea Research Part 2 Topical Studies in Oceanography* 103, 6–  
646 26.
- 647
- 648 Armbrecht, L. 2020. The potential of sedimentary ancient DNA to reconstruct past ocean  
649 ecosystems. *Oceanography*, <https://doi.org/10.5670/oceanog.2020.211>.
- 650
- 651 Armbrecht, L., Herrando-Pérez, S., Eisenhofer, R., Hallegraeff, G.M., Bolch, C.J.S., Cooper,  
652 A. 2020. An optimized method for the extraction of ancient eukaryote DNA from marine  
653 sediments. *Molecular Ecology Resources* 20, 906-919.
- 654
- 655 Armbrecht, L. Hallegraeff, G., Bolch, C.J.S., Woodward, C., Cooper, A. 2021. Hybridisation  
656 capture allows DNA damage analysis of ancient marine eukaryotes, *Scientific Reports* 11,  
657 3220.
- 658
- 659 Bennett, G. 1860 *Gatherings of a naturalist in Australasia*, Currawong Press, Australia,  
660 (1982) ISBN.
- 661
- 662 Blaauw, M., Christen J.A., Lopez, M.A., Vazquez J.E., Gonzalez O.M., Belding T., Theiler  
663 J., Gough, B., Karney, C. 2019. Age-Depth Modelling using Bayesian Statistics v. 2.3.6,  
664 <https://CRAN.R-project.org/package=rbacon>.
- 665
- 666 Blackburn, S.I., Bolch, C.J., Haskard, K.A., Hallegraeff, G.M. 2001. Reproductive  
667 compatibility among four global populations of the toxic dinoflagellate *Gymnodinium*  
668 *catenatum* (Dinophyceae). *Phycologia* 40, 78-87.
- 669
- 670 Bolch, C.J. and Hallegraeff, G.M., 1990. Dinoflagellate cysts in recent marine sediments  
671 from Tasmania, Australia. *Botanica Marina* 33, 173-192.
- 672
- 673 Bolch, C.J., Negri, A.P., Hallegraeff, G.M. 1999. *Gymnodinium microreticulatum* sp.nov.  
674 (Dinophyceae): a naked, microreticulate cyst producing dinoflagellate, distinct from  
675 *Gymnodinium catenatum* Graham and *Gymnodinium nolleri* Ellegaard et Moestrup.  
676 *Phycologia* 38, 301-313.
- 677
- 678 Bolch, C.J., Reynolds, M.J. 2002. Species resolution and global distribution of  
679 microreticulate  
680 dinoflagellate cysts. *Journal of Plankton Research* 24, 565-578.
- 681
- 682 Bolch, C.J., de Salas, M.F. 2007. A review of the molecular evidence for ballast water  
683 introduction of the toxic dinoflagellates *Gymnodinium catenatum* and the *Alexandrium*  
684 “*tamarensis* complex” to Australasia. *Harmful Algae* 6, 465-485.
- 685

- 686 Condie, S.A., Oliver, E.C.J., Hallegraeff, G.M. 2019. Environmental drivers of  
687 unprecedented *Alexandrium catenella* dinoflagellate blooms off eastern Tasmania, 2012–  
688 2018. *Harmful Algae* 87, 101628.  
689
- 690 Dela-Cruz, J., Ajani, P., Lee, R., Pritchard, T. and Suthers, I., 2002. Temporal abundance  
691 patterns of the red tide dinoflagellate *Noctiluca scintillans* along the southeast coast of  
692 Australia. *Marine Ecology Progress Series* 236, 75-88.  
693
- 694 Dela-Cruz, J., Middleton, J.H. and Suthers, I.M., 2003. Population growth and transport of  
695 the red tide dinoflagellate, *Noctiluca scintillans*, in the coastal waters off Sydney Australia,  
696 using cell diameter as a tracer. *Limnology and Oceanography* 48, 656-674.  
697
- 698 Gomes, H., Goes, J.I., Matodkar, S.G.P., Buskey, E.J., Basu, S., Parab, S., Thoppil, P. 2014.  
699 Massive outbreaks of *Noctiluca scintillans* blooms in the Arabian Sea due to spread of  
700 hypoxia. *Nature Communications* 5, 4862.  
701
- 702 Hallegraeff, G.M., Albinsson, M.E., Dowdney, J., Holmes, A.K., Mansour, M.P., Seger, A.  
703 2019. Prey preference, environmental tolerances and ichthyotoxicity by the red-tide  
704 dinoflagellate *Noctiluca scintillans* cultured from Tasmanian waters. *Journal of Plankton*  
705 *Research* 41, 407-418.  
706
- 707 Hallegraeff, G.M., Anderson, D.M., Belin, C., Bottein, M-Y., Bresnan, E., Chinain, M.,  
708 Enevoldsen, H., Iwataki, M., McKenzie, C.H., Sunesen, I., Pitcher, G.C., Provoost, P.,  
709 Richardson, A.J., Schweibold, L., Tester, P.A., Trainer, V.L., Yñiguez, A.T., Zingone, A.  
710 2021. Are harmful marine microalgal blooms and their societal impacts increasing? A 30 year  
711 global data analysis. *Nature Communications Earth & Environment* (in review).  
712
- 713 Hallegraeff, G.M, Bolch, C.J. 1992. Transport of diatom and dinoflagellate resting spores in  
714 ships' ballast water: implications for plankton biogeography and aquaculture. *Journal of*  
715 *Plankton Research* 14, 1067-1084.  
716
- 717 Hallegraeff, G.M., Schweibold, L., Jaffrezic, E., Rhodes, L., MacKenzie, L., Hay, B. and  
718 Farrell, H., 2020. Overview of Australian and New Zealand harmful algal species  
719 occurrences and their societal impacts in the period 1985 to 2018, including a compilation of  
720 historic records. *Harmful Algae*, 101848.  
721
- 722 Head, M.J., Lewis, J., De Vernal, A. 2006. The cyst of the calcareous dinoflagellate  
723 *Scrippsiella trifida*: Resolving the fossil record of its organic wall with that of *Alexandrium*  
724 *tamarensis*. *Journal of Paleontology* 80, 1-18.  
725
- 726 Herbig, A., Maixner, F., Bos, K.I., Zink, A., Krause, J. and Huson, D.H., 2016. MALT: Fast  
727 alignment and analysis of metagenomic DNA sequence data applied to the Tyrolean Iceman.  
728 *BioRxiv*, 050559.  
729

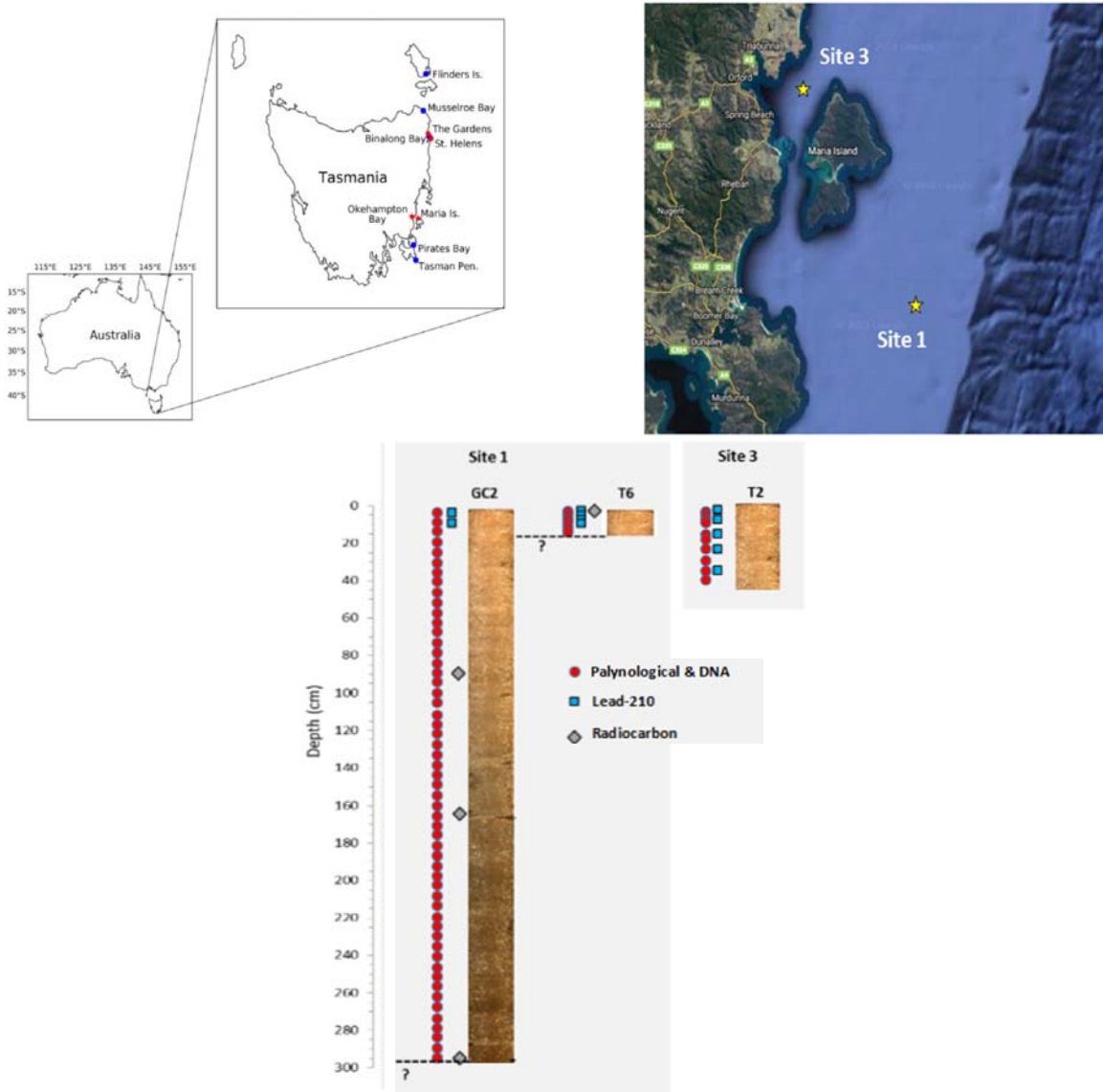
- 730 Hogg, A.G., Heaton, T.J., Hua, Q., Palmer, J.G., Turney, C.S., Southon, J., Bayliss, A.,  
731 Blackwell, P.G., Boswijk, G., Ramsey, C.B., Pearson, C. 2020. SHCal20 Southern  
732 Hemisphere Calibration, 0–55,000 years cal BP. *Radiocarbon* 62, 759-778.  
733
- 734 Horn, S. 2012. Target enrichment via DNA hybridization capture. In B. Shapiro and M.  
735 Hofreiter (Eds.), *Ancient DNA, methods and protocols* (pp. 177–188). New York, Dordrecht,  
736 Heidelberg, London: Springer.  
737
- 738 Hübler, R., Key, F.M., Warinner, C., Bos, K.I., Krause, J. and Herbig, A., 2019. HOPS:  
739 Automated detection and authentication of pathogen DNA in archaeological remains.  
740 *Genome Biology* 20, 1-13.  
741
- 742 Huson, D. H., Beier, S., Flade, I., Górská, A., El-Hadidi, M., Mitra, S., Tappu, R. 2016.  
743 MEGAN Community Edition - Interactive exploration and analysis of large-scale  
744 microbiome sequencing data. *PLOS Computational Biology* 12,  
745 e1004957. <https://doi.org/10.1371/journal.pcbi.1004957>.  
746
- 747 John, U., Alperman, T., Nagai, S., Litaker, R.W., Murray, S., Anderson, D.M., Bolch, C.,  
748 2018. Detailed insights into *Alexandrium catenella* (Dinophyceae) (Group 1 genotype)  
749 population structure and evolution. Abstracts 18th International Conference on Harmful  
750 Algae, Abstract Book. p. 324.  
751
- 752 John, U., Litaker, R.W., Montresor, M., Murray, S., Brosnahan, M.L., Anderson, D.M. 2014.  
753 Formal revision of the *Alexandrium tamarense* species complex (Dinophyceae) taxonomy:  
754 The introduction of five species with emphasis on molecular-based (rDNA) classification.  
755 *Protist* 165, 779-804.  
756
- 757 Jones, R., 1978. Why did the Tasmanians stop eating fish. In: Gould RA (ed), *Explorations in*  
758 *Ethno-Archaeology*, pp.11-47. University of New Mexico Press.  
759
- 760 Klouch, K.Z., Schmidt, S., Andrieux-Loyer, F., Le Gac, M, Hervio-Heath, D., Qui-Minet,  
761 Z.N., Quere J, Bigeard, E., Guillou, L., Siano, R. 2016. Historical records from dated  
762 sediment cores reveal the multidecadal dynamic of the toxic dinoflagellate *Alexandrium*  
763 *minutum* in the Bay of Brest (France). *FEMS Microbiology Ecology* 92, DOI  
764 10.1093/femsec/fiw101.  
765
- 766 McLeod, D. J., Hallegraeff, G. M., Hosie, G.W., Richardson, A. J. 2012. Climate driven  
767 range expansion of the red-tide dinoflagellate *Noctiluca scintillans* into the Southern Ocean.  
768 *Journal of Plankton Research* 34, 332–337.  
769
- 770 McMinn, A.1992. Recent and late Quaternary dinoflagellate cyst distribution on the  
771 continental shelf and slope of southeastern Australia. *Palynology* 16, 13-24.  
772

- 773 McMinn, A., Hallegraeff, G.M., Thompson, P., Jenkinson, A.V., Heijnis, H. 1998. Cyst and  
774 radionucleotide evidence for the recent introduction of the toxic dinoflagellate *Gymnodinium*  
775 *catenatum* into Tasmanian waters. Marine Ecology Progress Series 161,165-172.  
776
- 777 R Core Team. 2013. R: A language and environment for statistical computing. R Foundation  
778 for Statistical Computing, Vienna, Austria. URL <http://www.R-project.org/>.  
779
- 780 Ribeiro, S., Amorim, A., Andersen, T.J., Abrantes, F. and Ellegaard, M. 2012.  
781 Reconstructing the history of an invasion: the toxic phytoplankton species *Gymnodinium*  
782 *catenatum* in the Northeast Atlantic. Biological Invasions 14, 969-985.  
783
- 784 Ridgway, K. and Hill, K. 2009. Ridgway, K. and Hill, K. (2009) The East Australian Current.  
785 In A Marine Climate Change Impacts and Adaptation Report Card for Australia 2009 (Eds.  
786 E.S. Poloczanska, A.J. Hobday and A.J. Richardson), NCCARF Publication 05/09, ISBN  
787 978-1-921609-03-9.  
788
- 789 Ruvindy, R., Bolch, C.J., MacKenzie, L., Smith, K., Murray, S.A. 2018. qPCR assays for the  
790 detection and quantification of multiple paralytic shellfish toxin-producing species. Frontiers  
791 in Microbiology, DOI 10.3389/fmicb.2018.03153.  
792
- 793 Shaw, L.A., Weyrich, L.S., Hallegraeff, G.M., Cooper, A. 2019. Retrospective eDNA  
794 assessment of potentially harmful algae in historical ship ballast tank and marine port  
795 sediments. Molecular Ecology 28, 2476-2485.  
796
- 797 Stockmarr, J. 1971. Tablets with spores used in absolute pollen analysis. Pollen et Spores 13,  
798 615-621.  
799
- 800 Taylor, R., 2007. The polemics of eating fish in Tasmania: the historical evidence revisited.  
801 Aboriginal History 31, 1-26.  
802
- 803 Thompson, P.A., Baird, M.E., Ingleton, T., Doblin, M.A. 2009. Long-term changes in  
804 temperate Australian coastal waters: implications for phytoplankton. Marine Ecology  
805 Progress Series 394, 75–89.  
806
- 807 Thorsen, T., Dale, B., Nordberg, K. 1995. Blooms of the toxic dinoflagellate *Gymnodinium*  
808 *catenatum* as evidence of climate fluctuations in the late Holocene of southwest Scandinavia.  
809 The Holocene 5, 435-446.  
810
- 811 Trainer, V.L., Moore, S.K., Hallegraeff, G., Kudela, R.M., Clement, A., Mardones, J.I.,  
812 Cochrane, W.P. 2019. Pelagic harmful algal blooms and climate change: Lessons from  
813 nature’s experiments with extremes. Harmful Algae 91, 101591.  
814
- 815 Willerslev, E., Cooper, A. 2005. Ancient DNA. Proceedings of the Royal Society of London  
816 B: Biological Sciences 272, 3–16.

817

818 Yamaguchi, M., Itakura, S., Imai, I., Ishida, Y. 1995. A rapid and precise technique for  
819 enumeration of resting cysts of *Alexandrium* spp. (Dinophyceae) in natural sediments.

820 *Phycologia* 34, 207-214.



821

822

823

824

825

826 **Figure 1: Sediment coring sites near Maria Island, Tasmania, Australia.** Overview of

827 coring locations offshore (Gravity Core Site 1, GC2S1, and Multi-Core Site 1 Tube 6, MCS1-

828 T6, surface section only) and inshore Maria Island in the Mercury Passage (Multi-Core Site 3

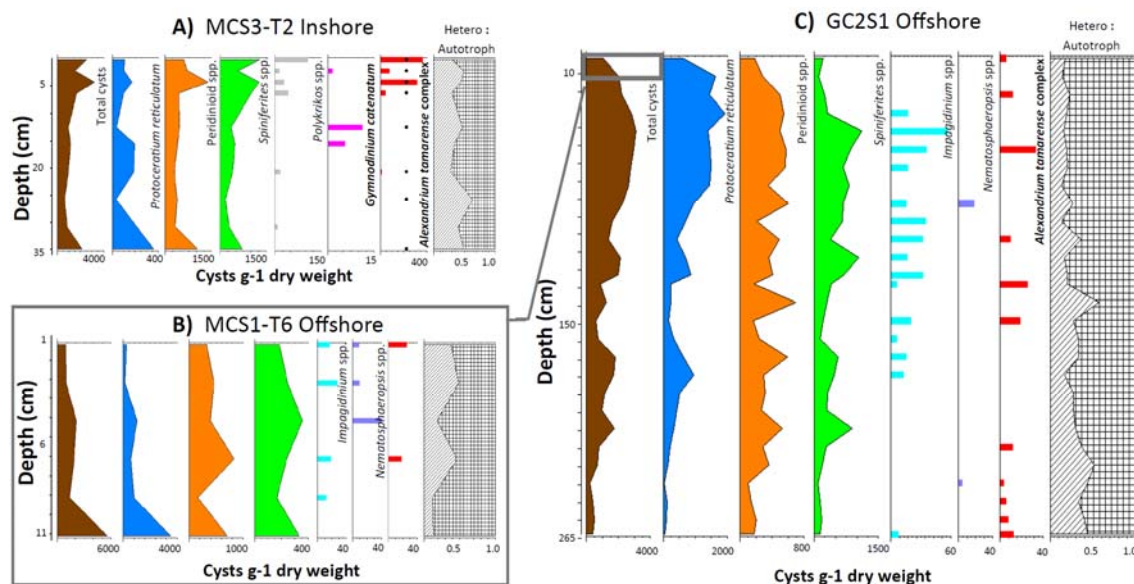
829 Tube 2, MCS3-T2). Red dots indicate palynology and *sedaDNA* sampling depths, blue

830 rectangles indicate Lead-210 ( $Pb^{210}$ ) dating sampling depths, and grey diamonds indicate

831 radiocarbon ( $^{14}C$ ) dating sampling depths.

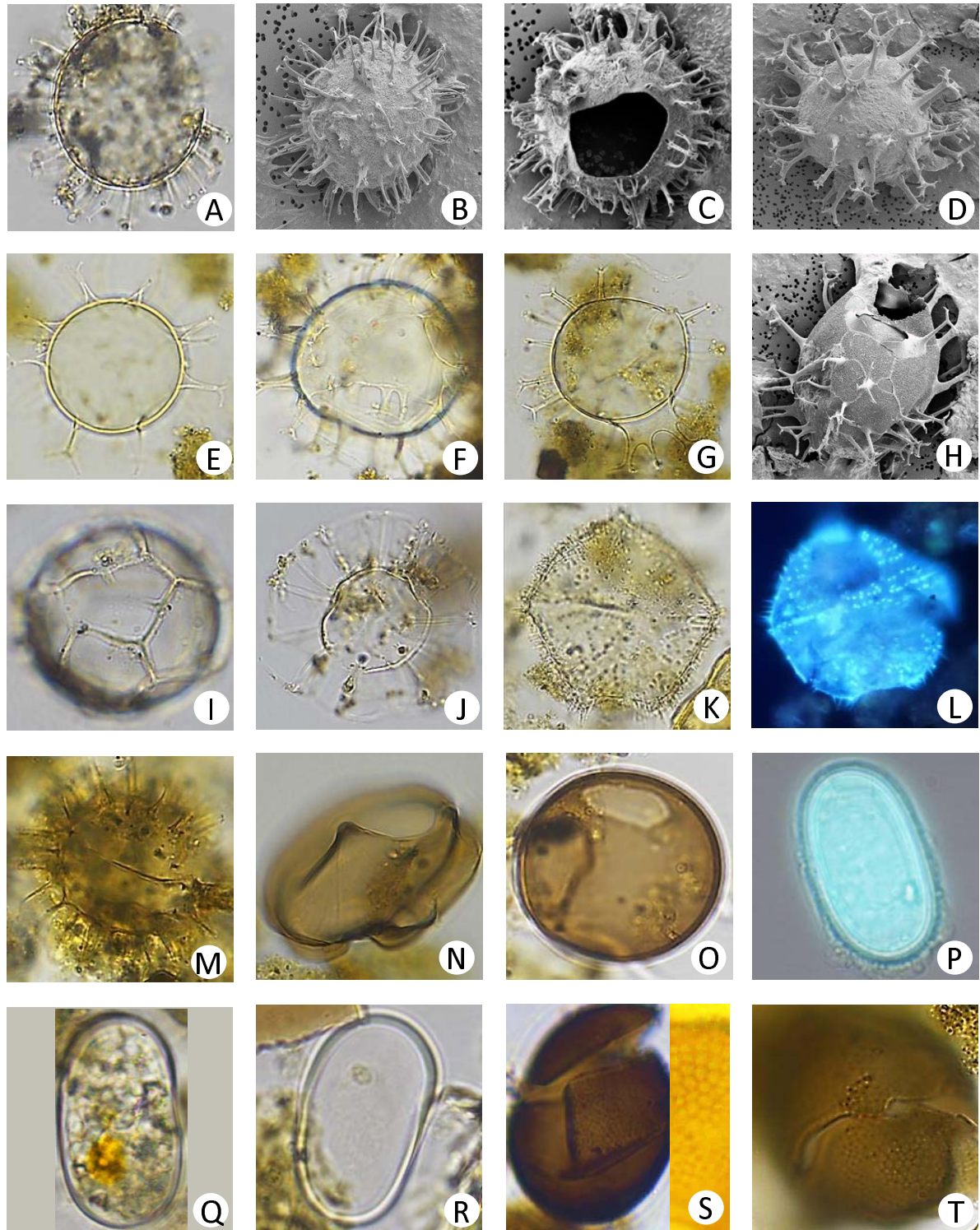
832

833



834  
835  
836  
837  
838  
839  
840  
841  
842

**Figure 2: Dinoflagellate cyst abundance at MCS3-T2 (inshore), and MCS1-T6 and GC2S1 (offshore) cores determined from palynological analyses.** Most abundant were cysts of *Protoceratium reticulatum*, *Spiniferites* and *Protoperidinium* species. *Impagidinium* and *Nematosphaeropsis* occurred offshore only, and *Polykrikos* and *Gymnodinium catenatum* were detected inshore only. *Alexandrium*-like cysts occurred both inshore and offshore. Cyst composition is also summarized as the ratio of heterotroph (mostly *Protoperidinium*) to autotroph taxa (mostly *Protoceratium*, *Spiniferites*).

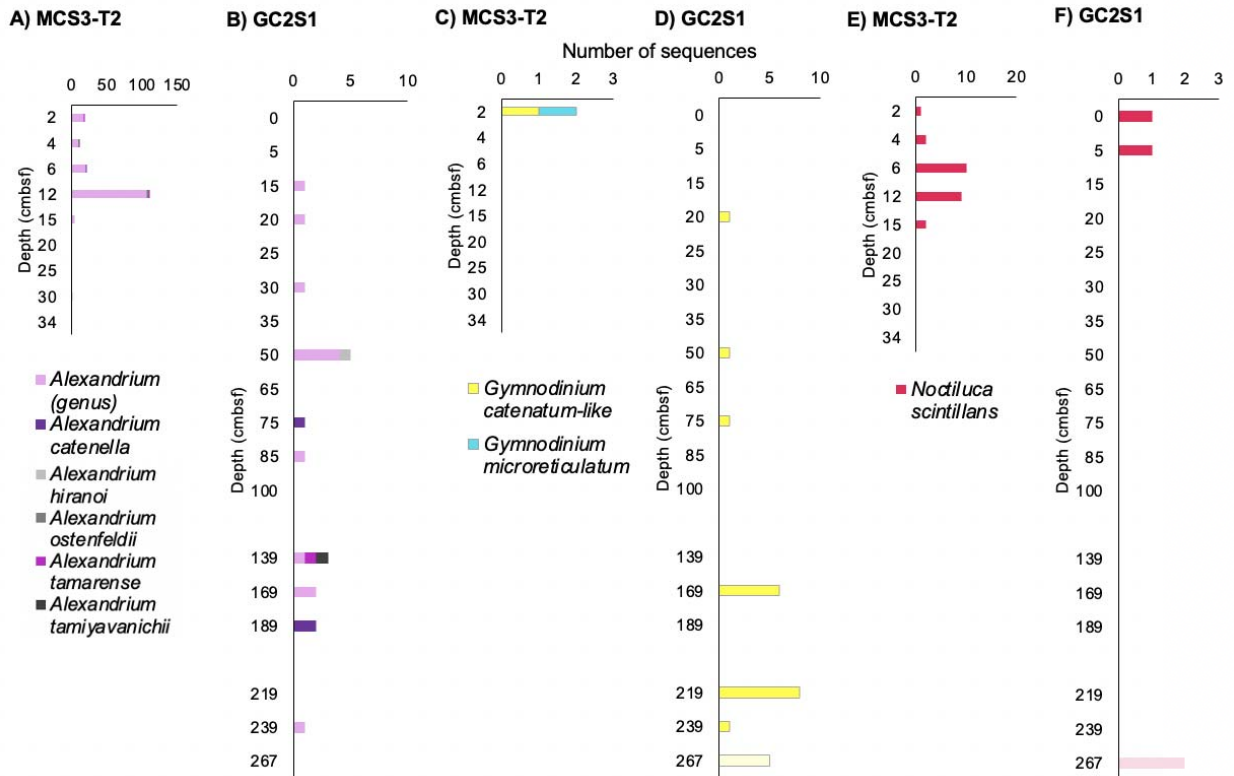


843

844

845 **Figure 3: Maria Island dinocysts.** A,B,C. Cysts of *Protoceratium reticulatum* with long  
846 processes (diameter 35 $\mu$ m), D,E.*Spiniferites bulloideus* (diameter 40 $\mu$ m), F. *Spiniferites*  
847 *hyperacanthus* (diameter 55 $\mu$ m); G: *Spiniferites mirabilis* (diameter 50 $\mu$ m), H: *Spiniferites*  
848 *ramosus* main body diameter 55 $\mu$ m), I: *Impagidinium sphaericum* (diameter 45 $\mu$ m., J:  
849 *Nematospaeropsis labyrinthus* (main body diameter 30  $\mu$ m); K,L: *Protoperidinium*

850 *shanghaiense* (length 70  $\mu\text{m}$ ), L. after primulin staining; . **M:** *Protoperidinium conicum* (main  
 851 body diameter 55  $\mu\text{m}$ ), **N:** *Protoperidinium subinermis* (diameter 55  $\mu\text{m}$ ), ), **O:**  
 852 *Protoperidinium avellana* (diameter 40  $\mu\text{m}$ ), **P,Q,R.** *Alexandrium tamarense* complex (length  
 853 35  $\mu\text{m}$ ), P. after primulin staining; T2 1cm; Q. live cyst with contents; R. T2 1cm ; **S:**  
 854 *Gymnodinium catenatum* (diameter 50  $\mu\text{m}$ ). + Detail of microreticulate ornamentation; **T:**  
 855 *Gymnodinium microreticulatum* (diameter 25  $\mu\text{m}$ )  
 856  
 857  
 858



859  
 860 **Figure 4: Abundance of *Alexandrium* spp., *Gymnodinium catenatum*-like species and**  
 861 ***Noctiluca scintillans* as determined by *sedaDNA* inshore and offshore Maria Island. A-**  
 862 **A-F) Normalized (rarefied) data derived after application of hybridization-capture using**  
 863 **HABbaits1. A,C,E) Inshore site MCS3-T2. B,D,F) Offshore site GC2S1. D,F) Light**  
 864 **colouring of bottom sample read counts indicates that contamination with modern sequences**  
 865 **cannot be excluded.**  
 866  
 867



868 **Table 1: *se*dDNA damage of reads assigned to the harmful dinoflagellate taxa *A.***  
869 ***catenella*, *G. catenatum*-like and *N. scintillans*.** The total number and proportion of reads  
870 classified into ancient and default via HOPS *se*dDNA damage analysis (based on HABbaits1  
871 data). The proportion of ancient reads is a measure of ‘% *se*dDNA damage’ for each of the  
872 three species (in italics).

| <b>Total</b>              | <b>GC2S1</b>   |                | <b>MCS3-T2</b> |                |
|---------------------------|----------------|----------------|----------------|----------------|
| <b>Taxa</b>               | <b>Ancient</b> | <b>Default</b> | <b>Ancient</b> | <b>Default</b> |
| <i>A. catenella</i>       | 13             | 19             | 0              | 6              |
| <i>G. catenatum</i> -like | 95             | 252            | 4              | 97             |
| <i>N. scintillans</i>     | 11             | 49             | 1              | 213            |
| <b>Proportion (%)</b>     | <b>GC2S1</b>   |                | <b>MCS3-T2</b> |                |
| <b>Taxa</b>               | <b>Ancient</b> | <b>Default</b> | <b>Ancient</b> | <b>Default</b> |
| <i>A. catenella</i>       | <i>41</i>      | <i>59</i>      | <i>0</i>       | <i>100</i>     |
| <i>G. catenatum</i> -like | <i>27</i>      | <i>73</i>      | <i>4</i>       | <i>96</i>      |
| <i>N. scintillans</i>     | <i>18</i>      | <i>82</i>      | <i>0.5</i>     | <i>99.5</i>    |

873